# Multiple-deme parallel genetic algorithm based on modular neural network for effective load shedding

**Ali Gholami-Rahimabadi**
Islamic Azad University East Tehran Branch
**Hadi Razmi** ( h_razmi@iauet.ac.ir )
Islamic Azad University East Tehran Branch https://orcid.org/0000-0003-3528-0164
**Hasan Doagou-Mojarrad**
Islamic Azad University East Tehran Branch

**Research Article**

**Keywords:** Load shedding, Multiple-deme parallel genetic algorithm, Neural network, Voltage stability

**Posted Date:** June 17th, 2021

**DOI:** https://doi.org/10.21203/rs.3.rs-390375/v1

**Noname manuscript No.**
(will be inserted by the editor)

# Multiple-deme parallel genetic algorithm based on modular neural network for effective load shedding

**Ali Gholami-Rahimabadi · Hadi Razmi · Hasan Doagou-Mojarrad**

Received: date / Accepted: date

**Abstract** One of the most effective corrective control strategies to prevent voltage collapse and instability is load shedding. In this paper, a multiple-deme parallel genetic algorithm (MDPGA) is used for a suitable design of load shedding. The load shedding algorithm is implemented when the voltage stability margin index of the power system is lower than a predefined value. In order to increase the computational speed, the voltage stability margin index is estimated by a modular neural network method in a fraction of a second. In addition, in order to use the exact values of the voltage stability margin index for neural network training, a simultaneous equilibrium tracing technique has been employed considering the detailed model of the components of the generating units such as the governor and the excitation system. In the proposed algorithm, the entire population is partitioned into several isolated subpopulations (demes) in which demes distributed in different processors and individuals may migrate occasionally from one subpopulation to another. The proposed technique has been tested on New England-39 bus test system and the obtained results indicate the efficiency of the proposed method.

**Keywords** Load shedding · Multiple-deme parallel genetic algorithm · Neural network · Voltage stability

## 1 Introduction

Recent blackouts related to voltage collapse around the world have significantly increased the importance of fast and accurate voltage stability assessment and control (Naganathan and Babulal, 2019; Suganyadevi et al., 2016). Generally, there are two ways to deal with voltage instability in power systems which are classified as preventive and corrective actions. Preventive actions are taken in a pre-contingency condition in order to increase the voltage stability margin while corrective actions are usually taken in a given post-contingency condition in order to restore system stability (Ahmadi and Alinejad-Beromi, 2015). One of the most effective corrective control tools (the latest solution) in facing voltage instability is load shedding (Mahari and Seyedi, 2016). There are two types of load shedding: under frequency load shedding (UFLS) and under voltage load shedding (UVLS) (Bakar et al., 2017; Sapari et al., 2018). In the former, the purpose of the UFLS is to quickly distinguish insufficiency of generation inside any system and automatically shed a lowest amount of the load until nominal frequency is restored whereas the UVLS refers to eliminating a specific amount of load of the power system in one or several points which is done following recognition of voltage instability and with a time delay. In fact, the UVLS problem is designed to determine where, when and how much of load should be eliminated until the power system conditions return to the previous or new equilibrium state and prevent voltage collapse and system blackout.

The best load shedding scheme should be able to find the feasible and most economical plan for determining optimal load shedding in the shortest time by considering power system constraints (Hooshmand and Moazzami, 2012). In literature, many different algorithms regarding load shedding schemes using frequency and voltage as a criterion have been proposed. In (Aman et al., 2019), a novel load shedding scheme based on voltage and center of inertia frequency (COIF) through simulation on PSCAD/EMTDC is proposed. In order to operate load shedding, globalized COIF, change in reactive power and bus voltages as locally are calculated. In (Javadi and Amraee, 2018), mixed integer programming-based under voltage load shedding (UVLS) model is investigated to find the amount of load shedding according to the value of loading margin.

Ali Gholami-Rahimabadi
Department of Electrical Engineering, East Tehran Branch, Islamic Azad University, Tehran, Iran

Hadi Razmi (Corresponding author)
Department of Electrical Engineering, East Tehran Branch, Islamic Azad University, Tehran, Iran
Tel.: +98-21-33594950-59
Fax: +98-21-33584011
E-mail: h_razmi@iauet.ac.ir

Hasan Doagou-Mojarrad
Department of Electrical Engineering, East Tehran Branch, Islamic Azad University, Tehran, Iran

The distributed load shedding technique based on two-level framework is presented in (Tian and Mou, 2019). The local load shedding controllers in low-level and the upper one is used to reduce the amount of load shedding. In (Nojavan et al., 2017) a new power market approach based on optimal arrangement of curtailable loads (CLs) in order to secure the desired VSM for the heavily-loaded power grids, is proposed. The minimization of the summation of the power generation and curtailment costs are considered as objective function. In (Jalali et al., 2019) an optimal transmission line switching as a new facility for economic improvement of VSM is presented. The other preventive control facilities including demand response, active/reactive generation rescheduling and load shedding is considered for economic improvement of VSM. In (Li et al., 2018) a fuzzy load-shedding strategy considering the impact of photovoltaic cell (PV) output fluctuations is presented. In this paper, the load bus voltage amplitude, load margin index and the load-shedding command are fuzzy input and output variables, respectively. In (Modarresi et al., 2018), a new adaptive neuro-fuzzy inference system (ANFIS) and centralized UVLS based on local measurement using phasor measurement units (PMUs) is proposed to estimate the amount of load shedding. Three case studies are considered by DigSILENT Power Factory. Also, a probabilistic UVLS scheme using the power flow equations considering heuristic optimization methods is proposed in (Kaffashan and Amraee, 2015). In the paper, short-term voltage instability and the effect of dynamic devices were not be taken into account. To overcome these problems, the voltage stability index (VSI)-based UVLS methods have been proposed in the literature. The required data of VSI-based methods can be extracted from different sources such as power flow equations, time-domain simulation and the wide-area measurement system (WAMS) (Lei et al., 2014). A comprehensive review of these VSIs is given in (Modarresi et al., 2016). In (Shekari et al., 2016), a new centralized adaptive load shedding scheme based on both frequency and voltage stability assessments is proposed in three stages: 1) data required for implementation of the proposed method, 2) post load shedding strategies based on operational limitations and voltage stability criteria, and 3) with respect to event type in real time, pre-specified optimal load shedding scheme and post load shedding strategies are implemented. Recently, computational intelligence-based techniques have been proposed in the application of load shedding problem such as Differential Evolution (DE) (Arya et al., 2012a; Titare et al., 2014; Xu et al., 2013; Arya et al., 2012b), Particle Swarm Optimization (PSO) (Hosseini-Bioki et al., 2013; Hazra and Sinha, 2007; Amraee et al., 2007), Genetic Algorithm (GA) (Kanimozhi et al., 2014; Tamilselvan and Jayabarathi, 2016; Khamis et al., 2018), Particle Swarm-Based-Simulated Annealing Optimization (PSO-B-SA) (Sadati et al., 2009), Hybrid Imperialist Competitive Algorithm-Pattern Search (HICA-PS) (Moazzami et al., 2016), Discrete Imperialistic Competition Algorithm (DICA) (Mahari and Seyedi, 2016), Grey Wolf Optimizer (GWO) (Mahdad and Srairi, 2015), Glowworm Swarm Optimization (GSO) (Mageshvaran and Jayabarathi, 2015a), Immune System Reinforcement Learning-Based (ISRL-Based) algorithm (Babalola et al., 2017), alternating optimization method (Xia et al., 2016), Big Bang-Big Crunch (BB-BC) method (Kucuktezcan and Genc, 2015), Improved Harmony Search Algorithm (IHSA) (Mageshvaran and Jayabarathi, 2015b), and Teaching Learning Based Optimization (TLBO) (Arya and Koshti, 2014).

Table 1 shows the comparison of our load shedding strategy with other methods investigated in the published papers.

The technique suits well for online voltage stability assessment and control if it accurately indicates voltage stability margin of power system and it should be fast enough to accomplish corrective actions. Therefore, the mentioned load shedding techniques usually have the following drawbacks:

- These techniques use traditional load flow algorithms to calculate various voltage stability indices of the power system. The descriptions of generators in traditional load flow are very different from their actual dynamic response. The behavior of generators in a dynamic process depends on the dynamic characteristics of the synchronous machine and its control systems such as the governor. In traditional load flow, these controls are not defined for power system generators, so that the bus slack generator is modeled as constant voltage amplitude and angle and other generators by constant voltage amplitude (Lim and Mustafa, 2016). Therefore, the voltage stability indices obtained to traditional load flow methods are not calculated precisely.
- Computational intelligence-based techniques mainly use iterative-based optimization algorithms to execute load shedding strategies, and the most significant defect of this method that it is considerably time-consuming. As a result, these techniques are not suitable for this purpose.

In this paper, a load shedding strategy based on multiple-deme parallel genetic algorithm (MDPGA) has been designed and developed. Compared to the other evolutionary techniques, the major advantages of MDPGA are: its higher speed and efficiency, maintaining the diversity of the population, the ability to find global and local minimums, minimal storage requirement and additional CPU availability. In addition, to increase the calculation speed of the voltage stability index for each chromosome, a modular neural network which is capable of mapping the power system operating conditions and the voltage stability margin index, is used. Also, to generate the neural network training database, simultaneous equilibrium tracing technique has been applied. This method accurately calculates the voltage stability margin by detailed modeling of the generating units and solving the algebraic-differential equations of the power system in the steady-state.

As a result, the main contributions of the study can be summarized as follows:

- **Accurate calculating of voltage stability margin index using simultaneous equilibrium tracing technique:** So far, load shedding studies based on steady state voltage stability assessment have not been addressed, which simultaneously considers all AVR voltage limits and calculates both SNB and SLIB points. Therefore, in this paper, a new robust methodology based on the predictor-corrector method is proposed to accurately calculate the steady state volt-

**Table 1** Comparison of the proposed load shedding method with other published papers.

| | | |
|---|---|---|
| **Our method** | Technique | Multiple-deme parallel genetic algorithm based on modular neural network |
| | Test system | New England-39 bus test system |
| | Power system model | The generators are modeled in detail and all AVR voltage limits are considered |
| | Voltage stability index | Voltage stability margin (VSM) obtained by neural network |
| | Objective function | Minimize the amount of load shed |
| (Javadi and Amraee, 2018) | Technique | Mixed integer programming (MIP) |
| | Test system | IEEE 14 and 118 bus test systems |
| | Power system model | Relies on power flow models |
| | Voltage stability index | Loading margin (LM) |
| | Objective function | Minimize the total load curtailment with considering load priorities |
| (Sadati et al., 2009) | Technique | Global particle swarm-based-simulated annealing (PSO-SA) optimization |
| | Test system | IEEE 14 and 118 bus test systems |
| | Power system model | Relies on power flow models |
| | Voltage stability index | Voltage stability margin (VSM) obtained by repetitive power flow algorithms |
| | Objective function | Minimize the interruption cost |
| (Hosseini-Bioki et al., 2013) | Technique | PSO |
| | Test system | IEEE three-bus and modified 30-bus test system |
| | Power system model | Relies on power flow models |
| | Voltage stability index | Loadability limit obtained by repetitive power flow algorithms |
| | Objective function | Minimize the congestion rent and maximize the system loadability |
| (Tamilselvan and Jayabarathi, 2016) | Technique | Hybrid genetic algorithm and neural network |
| | Test system | IEEE six and 14 bus test systems |
| | Power system model | Relies on power flow models |
| | Voltage stability index | Voltage stability risk index (VSRI) obtained by repetitive power flow algorithms |
| | Objective function | Minimize the total load shed and maximize the voltage stability |
| (Jalali et al., 2019) | Technique | Modified PSO |
| | Test system | IEEE 39-bus test system |
| | Power system model | Relies on power flow models |
| | Voltage stability index | Voltage stability margin (VSM) obtained by repetitive power flow algorithms |
| | Objective function | Minimize the power generation and curtailment costs |
| (Li et al., 2018) | Technique | Fuzzy strategy |
| | Test system | IEEE 14-bus system |
| | Power system model | Ordinary differential equations (ODEs) |
| | Voltage stability index | Load margin index obtained by repetitive power flow algorithms |
| | Objective function | Minimize the load shedding quantity |
| (Nojavan et al., 2017) | Technique | Hybrid non-linear programming and modified binary PSO |
| | Test system | IEEE 118-bus test system |
| | Power system model | Relies on power flow models |
| | Voltage stability index | Voltage stability margin (VSM) obtained by repetitive power flow algorithms |
| | Objective function | Minimize the cost of preventive control facilities |

age stability margin index. In this method, the generating units are modeled in detail and the algebraic-differential equations of the power system are solved in a steady state.

- **Fast estimating of voltage stability margin index using modular neural network method:** For online voltage stability studies, a suitable indicator that has two characteristics: 1) accurately shows the voltage stability margin of the power system; 2) calculated fast enough to implement corrective actions such as load shedding. The simultaneous equilibrium tracing technique relies on power flow models to calculate the voltage stability margin index. This method has a long computational time problem due to the use of repetitive power flow algorithms. Therefore, the voltage stability margin indices of the limited power system obtained by the simultaneous equilibrium tracing technique were used to train the modular neural network method in order to quickly estimate the voltage stability margin index.
- **Using multiple-deme parallel genetic algorithm (MDPGA) with parallel processing capability for faster and more economical implementation of load shedding strategy:** Compared to the other evolutionary techniques, the major advantages of MDPGA are: its higher speed and efficiency, maintaining the diversity of the population, the ability to find global and local minimums, minimal storage requirement and additional CPU availability. In addition, to increase the implementation speed of the load shedding strategy, a modular neural network which is capable of mapping the power system operating conditions and the voltage stability margin index, is used for each chromosome.

The present article includes the following sections:
Section 2 presents the mathematical formulation of load shedding problem as a constrained optimization problem by considering equality and inequality constraints. Section 3 contains voltage stability margin estimation using modular neural network method. Section 4 describes the load shedding algorithm with multiple-deme parallel genetic algorithm. The obtained numerical results from proposed method will be presented in section 5.

## 2 Mathematical formulation

Generally, the problem of load shedding can be expressed as constrained nonlinear optimization problem. The main objective function is to minimize total amount of the load to be shed at the current operating condition. Symbolically, it is represented as

$$\text{minimize} \quad Obj = \sum_{i=1}^{l} b_i \times P_{shd_i} \tag{1}$$

where, $l$ is the number of power system load buses, $b_i$ is the binary decision variable to status of the $i$th load bus, and $P_{shd_i}$ is the amount of active power shed of the $i$th load bus ($P_{shd_i} = 0.01 \times \alpha_i \times P_{L_i}$). $P_{L_i}$ is the active power of the $i$th load bus and $\alpha_i$ is the percentage of load can be shed in the $i$th load bus. The minimization of the above objective function is subjected to the following equality and inequality constraints.

### 2.1 The equality constraints

Unlike in power flow analysis, a detailed representation of different components of the power system is required to accurately analyze the system's behavior. When the differential and algebraic equations of the power system is expressed by $\dot{\boldsymbol{x}} = \boldsymbol{F}(\boldsymbol{x}, \boldsymbol{y}, \boldsymbol{u}, \boldsymbol{z})$ and $\boldsymbol{0} = \boldsymbol{G}(\boldsymbol{x}, \boldsymbol{y}, \boldsymbol{u}, \boldsymbol{z})$, respectively; these equations in the steady-state ($\dot{\boldsymbol{x}} = \boldsymbol{0}$), represent the set of equality constraints for the optimization problem.

Without the loss of generality, it is assumed that the power system has $n$ buses and $m$ two-axis synchronous generators; each generator is equipped with the simplified IEEE type DC-1 excitation system (Rahman et al., 2021), a simplified prime mover and speed governor. If the remaining components of the power system are represented by their power flow models, then all of the equality constraints can be summarized as follows (Razmi et al., 2012):

$$(\omega_i - \omega_m)\omega_0 = 0; \quad i = 1, \cdots, m-1 \tag{2}$$

$$M_i^{-1}\left[P_{m_i} - D_i(\omega_i - \omega_m) - (E'_{q_i} - X'_{d_i} I_{d_i}) I_{q_i} - (E'_{d_i} + X'_{q_i} I_{q_i}) I_{d_i}\right] = 0; \quad i = 1, \cdots, m \tag{3}$$

$$T_{d0}^{-1}\left[E_{fd_i} - E'_{q_i} - (X_{d_i} - X'_{d_i}) I_{d_i}\right] = 0; \quad i = 1, \cdots, m \tag{4}$$

$$T_{q0}^{-1}\left[-E'_{d_i} + (X_{q_i} - X'_{q_i}) I_{q_i}\right] = 0; \quad i = 1, \cdots, m \tag{5}$$

$$T_{e_i}^{-1}\left[V_{r_i} - (K_{e_i} + S_{e_i}) E_{fd_i}\right] = 0; \quad i = 1, \cdots, m \tag{6}$$

$$T_{a_i}^{-1}\left[-V_{r_i} + K_{a_i}(V_{ref_i} - V_i - R_{f_i})\right] = 0; \quad i = 1, \cdots, m \tag{7}$$

$$T_{f_i}^{-1}\left[-R_{f_i} - (K_{e_i} + S_{e_i}) K_{f_i} E_{fd_i} T_{e_i}^{-1} + K_{f_i} V_{r_i} T_{e_i}^{-1}\right] = 0; \quad i = 1, \cdots, m \tag{8}$$

$$T_{ch}^{-1}\left[\mu_i - P_{m_i}\right] = 0; \quad i = 1, \cdots, m \tag{9}$$

$$T_{g_i}^{-1}\left[P_{G_i} - (\omega_i - \omega_{ref_i}) R_i^{-1} - \mu_i\right] = 0; \quad i = 1, \cdots, m \tag{10}$$

where,

$$I_d = \left[R_s^2 + X'_d X'_q\right]^{-1}\left[R_{s_i} E'_d + E'_q X'_q - R_{s_i} V_i \sin(\delta_i - \theta_i) - X'_q V_i \cos(\delta_i - \theta_i)\right] \tag{11}$$

$$I_d = \left[R_s^2 + X'_d X'_q\right]^{-1}\left[R_{s_i} E'_q + E'_d X'_d - R_{s_i} V_i \cos(\delta_i - \theta_i) + X'_d V_i \sin(\delta_i - \theta_i)\right] \tag{12}$$

Furthermore, the network power balance equations can be written as follows:

$$I_{d_i} V_i \sin(\delta_i - \theta_i) + I_{q_i} V_i \cos(\delta_i - \theta_i) - P_{L_i}^{new} - \sum_{k=1}^{n} V_i V_k y_{ik} \cos(\theta_i - \theta_k - \gamma_{ik}) = 0; \quad i = 1, \cdots, n \tag{13}$$

$$I_{d_i} V_i \cos(\delta_i - \theta_i) - I_{q_i} V_i \sin(\delta_i - \theta_i) - Q_L^{new} - \sum_{k=1}^{n} V_i V_k y_{ik} \sin(\theta_i - \theta_k - \gamma_{ik}) = 0; \quad i = 1, \cdots, n \tag{14}$$

where, $P_L^{new} = P_{L_i} - P_{Shd_i}$ and $Q_L^{new} = Q_{L_i} - Q_{Shd_i}$. $Q_{L_i}$ is the reactive power of the $i$th load bus and $Q_{Shd_i}$ is the amount of reactive power shed of the $i$th load bus. Other parameters and variables of Eqs. (2)-(14) are defined in (Razmi et al., 2012).

Also, it is assumed that during the implementation of load shedding the power factor is constant. Therefore, the following equality constraint must also be satisfied:

$$Q_{Shd_i} = \frac{Q_{L_i}}{P_{L_i}} P_{Shd_i}; \quad i = 1, \cdots, l \tag{15}$$

In (2)-(14), the state vector $\boldsymbol{x}$, algebraic vector $\boldsymbol{y}$, control vector $\boldsymbol{u}$ and parameter vector $\boldsymbol{z}$ contain the following variables:

$$\begin{aligned}\boldsymbol{x} &= [\delta_1, \cdots, \delta_{m-1}, \omega_1, \cdots, \omega_m, E'_{q_1}, \cdots, E'_{q_m}, E'_{d_1}, \cdots, E'_{d_m}, P_{m_1}, \cdots, P_{m_m}, \\ &\quad \mu_1, \cdots, \mu_m, E_{fd_1}, \cdots, E_{fd_m}, V_{r_1}, \cdots, V_{r_m}, R_{f_1}, \cdots, R_{f_m}]^T \\ \boldsymbol{y} &= [V_1, \cdots, V_n, \theta_1, \cdots, \theta_n]^T \\ \boldsymbol{u} &= [P_{G_1}, \cdots, P_{G_m}, V_{ref_1}, \cdots, V_{ref_m}, \omega_{ref_1}, \cdots, \omega_{ref_m}]^T \\ \boldsymbol{z} &= [P_{L_1}, \cdots, P_{L_l}, Q_{L_1}, \cdots, Q_{L_l}]^T\end{aligned} \tag{16}$$

It is noted that the $m$th generator's rotor angle is selected as the power system angle reference.

### 2.2 The inequality constraints

The inequality constraints of the optimization problem include the following:

- The steam valve or water gate opening of governors:

$$\mu_i^{min} \le \mu_i \le \mu_i^{max}; \quad i = 1, \cdots, m \tag{17}$$

  where, $\mu_i^{min}$ and $\mu_i^{max}$ are the lower and upper limits of $\mu_i$, respectively.

- The output of automatic voltage regulators (AVRs):

$$V_r^{min} \le V_{r_i} \le V_r^{max}; \quad i = 1, \cdots, m \tag{18}$$

  where, $V_{r_i}^{min}$ and $V_{r_i}^{max}$ are the minimum and maximum limits of $V_{r_i}$, respectively.

- The voltage of load buses (Lee et al., 2015):

$$V_i^{min} \le V_i \le V_i^{max}; \quad i = 1, \cdots, l \tag{19}$$

  where, $V_i^{min}$ and $V_i^{max}$ are the lower and upper limits of $V_i$, respectively.

- The voltage stability margin of the power system:

$$vsm \ge vsm^{min} \tag{20}$$

  where, $vsm$ is the voltage stability margin index and $vsm^{min}$ is the lower limit of $vsm$.

- The percentage of load can be shed:

$$\alpha_i^{min} \le \alpha_i \le \alpha_i^{max}; \quad i = 1, \cdots, l \tag{21}$$

  where, $\alpha_i^{min}$ and $\alpha_i^{max}$ are the minimum and maximum limits of $\alpha_i$, respectively.

It should be noted that the state and algebraic variables can be solved simultaneously by directly applying Newton's method to the differential and algebraic equations of the power system in steady-state. Moreover, the voltage stability index is estimated by the neural network method explained in more details in the next section. Also, the above equality and inequality constraints except (15) and (21) should be maintained under the current operating condition ($P_{Shd_i} = 0$) as well as next predicted load condition accounting load shed. Constraints (15) and (21) are only related to the current operating condition.

## 3 The voltage stability margin estimation

For operational purposes in which the fast responses are of crucial importance, using the neural network method seems a better approach. Hence, a modular neural network method with the following model and specification is used here to estimate the voltage stability margin of the power system:

1. Different configurations are considered for the power system. In configuration 1, all transmission lines are energized. Other configurations are produced by outage of one transmission line. For each configuration, one module is assigned to learn its training data.
2. Each module is a multi-layer perceptron network with one hidden layer.
3. In each configuration, several loading levels are considered by changing the active power of load buses randomly. The change in loads is distributed among the participating generators, and their designated real power generation changes in proportion to their participation factors in the base case.
4. Using the simultaneous equilibrium tracing technique described in details in (Razmi et al., 2012), at each loading level of a specific power system configuration, a pattern is generated for the corresponding neural network module.

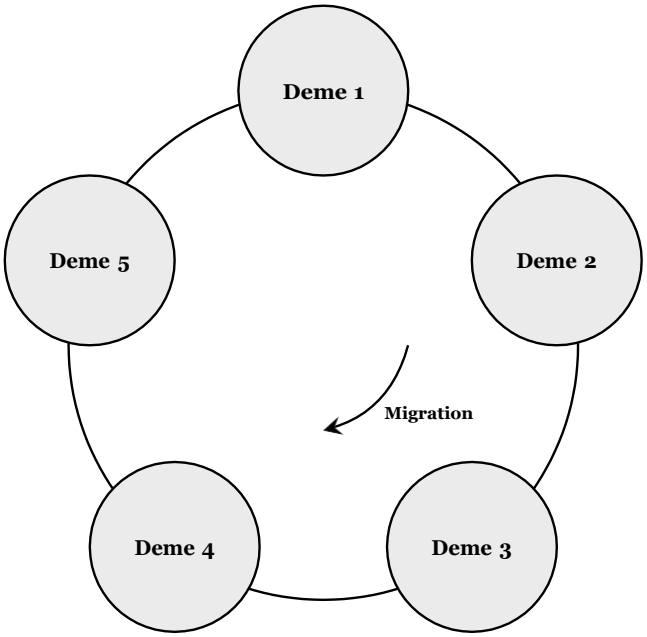


**Fig. 1** Ring topology of multiple-deme parallel genetic algorithm.

5. Modules have $n+3m+2l$ neurons in the input layer for active and reactive powers of load buses, designated real power generation, voltage output of AVRs, transient direct axis and quadrature axis EMF of generators and PQ bus voltages.
6. Modules have one neuron in the output layer for the voltage stability margin index of the power system. This index is obtained from the difference of the total active load of the power system at the critical point where voltage collapse associated with the saddle node bifurcation (SNB) or the saddle limit induced bifurcation (SLIB) occurs and the initial conditions (Razmi et al., 2012).
7. The number of neurons in the hidden layer is selected by trial and error method.
8. The unipolar sigmoid activation function is used for hidden and output neurons.
9. The mean squared error is considered as the neural network performance function.
10. Both input and output variables of the neural network are normalized between 0 and 1.
11. Levenberg-Marquardt training algorithm is used for weights and biases updating.
12. Each module of the neural network is trained until a determined termination criterion is achieved.

## 4 The load shedding algorithm

In this paper, a multiple-deme parallel genetic algorithm is used for load shedding. Multiple-deme parallel genetic algorithms are the extension of traditional single-population genetic algorithms (SPGAs) (dos Santos Coelho and Mariani, 2007; Bora et al., 2019) that can be considered as a class of parallel processing methods. Higher speed and efficiency, additional CPU availability, more resistance to premature convergence and maintaining larger diversity are advantages of this algorithm in comparison to the traditional single-population genetic algorithm (Asrari et al., 2016; Dey et al., 2019). In the multiple-deme parallelization scheme, the entire population is partitioned into several isolated subpopulations (demes) in which demes are distributed in different processors and individuals may migrate occasionally from one subpopulation to another. Despite the advantages mentioned, the way to choose the parameters of the multiple-deme parallel genetic algorithm, such as migration rate, migration interval, connection topology, migration policy, and population size, greatly affect its performance. Different migration topologies such as star, ring, torus, hypercube and 2D/3D mesh can be used to move individuals from one subpopulation to another. In this study, the ring topology with five subpopulations and the best-worst migration policy is used (Wang and Singh, 2009). The migration between two neighbors in this topology is considered clockwise (Wang and Singh, 2009). Note that migration rate should be in a way that the number of main individuals in each subpopulation is more than the number of new individuals migrated to it. In Fig. 1, the proposed topology is shown. If the voltage stability margin estimated by the neural network module associated with the power system configuration does not satisfy the constraint (20) at the current operating condition, the load shedding algorithm based on multiple-deme parallel genetic algorithm is implemented. The proposed algorithm is shown in Fig. 2.
The steps of implementing the load shedding algorithm are as follows:

- **Initial population generation:** Initial population with $n_{pop}$ chromosomes is randomly generated. The chromosomes are represented in the binary encoding system. Each chromosome has two parts. The first part of each chromosome

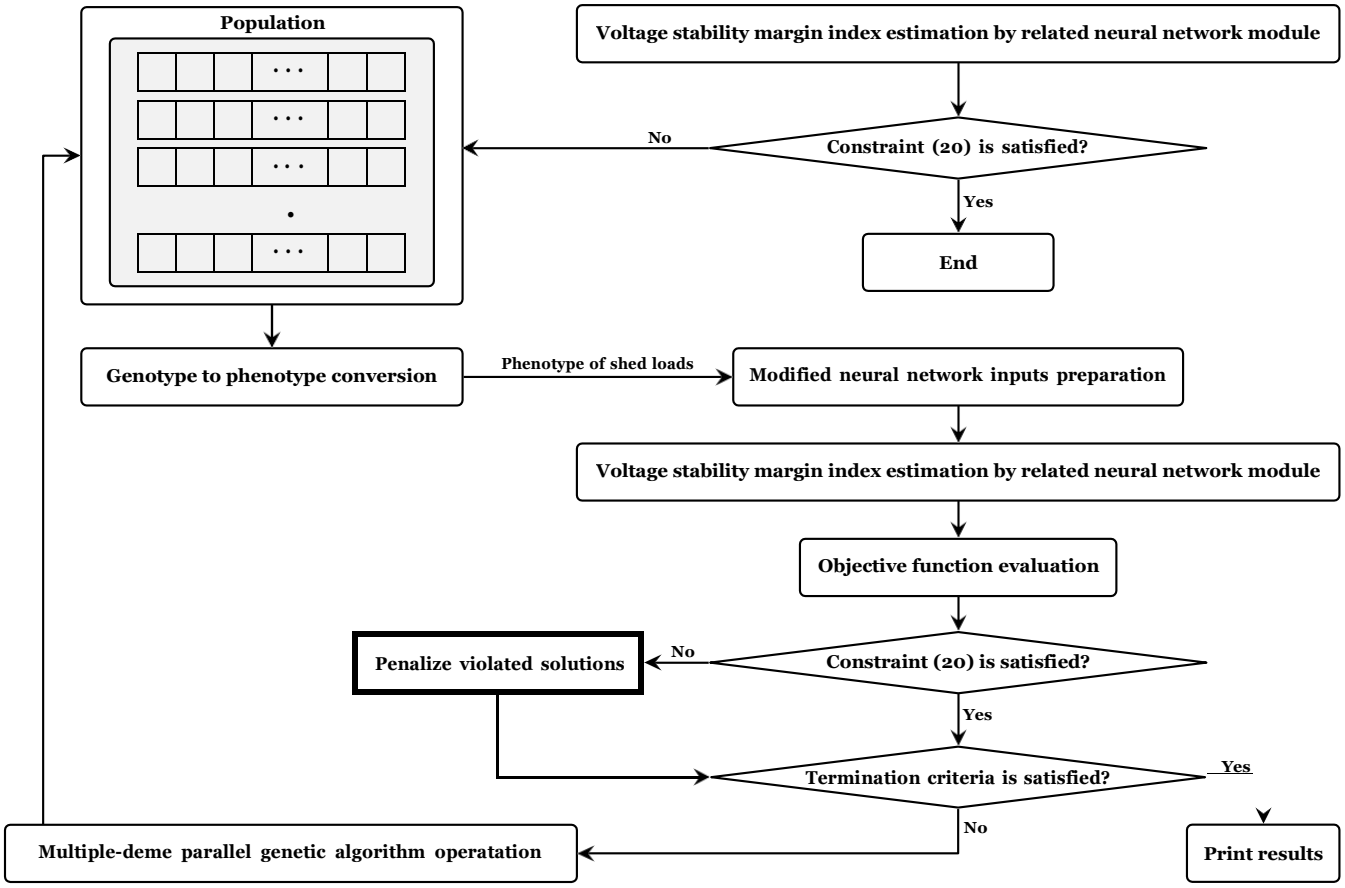


**Fig. 2** The control block diagram.

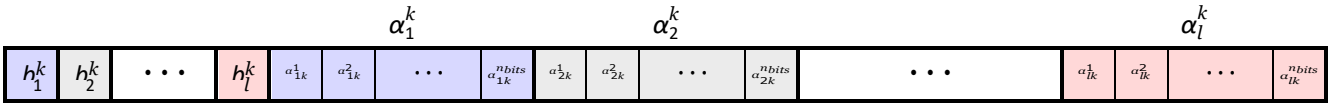

**Fig. 3** Chromosome representation.

has $l$ bits and each bit indicates the participation or non-participation of the corresponding bus in the load shedding program. The second part comprises strings in number of candidate buses for load shedding and each string equals percentage of load to be shed in the corresponding bus. Depending on the required calculation accuracy, the number of bits in each string ($n_{bits}$) is determined. In this manner, the $k$th chromosome of the population is represented as shown in Fig. 3.

- **Genotype to phenotype conversion:** Eq. (22) is used for converting genotype to phenotype of the $i$th string in the second part of the $k$th individual.

$$\alpha_i^k = \alpha_i^{min} + \frac{\alpha_i^{max} - \alpha_i^{min}}{2^{n_{bits}} - 1} \times d_i^k \tag{22}$$

where, $d_i^k$ is the decimal value of the $i$th string in the second part of the $k$th individual.

- **Modified neural network inputs preparation:** The values of the following variables are calculated as neural network inputs according to the equations described in section 4.1 of reference (Razmi et al., 2012).

$$P_{L_i} - P_{shd_i},\ Q_{L_i} - Q_{shd_i};\quad i = 1, \cdots, l$$
$$P_{G_i},\ V_{r_i},\ E_{d_i}',\ E_{q_i}';\quad i = 1, \cdots, m$$
$$V_i;\quad i = 1, \cdots, n_{pq}\quad (n_{pq} = n - m)$$

- **Voltage stability margin estimation:** After preparing the neural network inputs, the voltage stability margin index of the power system is estimated by the method presented in the previous section.

**Table 2** The configurations considered in the power system.

| Configuration | Description | $n$ | $l$ | $m$ |
|---|---|---|---|---|
| C1 | Normal case (all transmission lines are energized) | 39 | 18 | 10 |
| C2 | Outage of line 16-19, load 20 and generators 33 and 34 | 35 | 17 | 8 |
| C3 | Outage of line 6-31 and generator 31 | 38 | 18 | 9 |
| C4 | Outage of line 10-32 and generator 32 | 38 | 18 | 9 |
| C5 | Outage of line 22-35 and generator 35 | 38 | 18 | 9 |
| C6 | Outage of line 19-33 and generator 33 | 38 | 18 | 9 |
| C7 | Outage of line 19-20, load 20 and generator 34 | 37 | 17 | 9 |
| C8 | Outage of line 23-36 and generator 36 | 38 | 18 | 9 |
| C9 | Outage of line 25-37 and generator 37 | 38 | 18 | 9 |
| C10 | Outage of line 2-30 and generator 30 | 38 | 18 | 9 |

- **Objective function evaluation:** Calculate the value of the objective function for the $k$th chromosome ($Obj^k$) using Eq. (1). If the index estimated in the previous step satisfies the constraint (20), the penalty value is equal to zero and otherwise a very large positive number will be considered. Finally, the value of the objective function for the $k$th chromosome is calculated by the following equation:

$$Obj^k = Obj^k + penalty \tag{23}$$

- **Check termination criterion:** If the algorithm termination criterion is satisfied, the amount of load shedding in candidate buses are identified; otherwise, by applying migration, selection, crossover and mutation, steps 2-6 are repeated.

## 5 Simulation results

The proposed method has been tested on the New England 39-bus power system. The data related to this power system is available in (Razmi et al., 2012). It is assumed that in this article, all load buses are candidates for load shedding. The different configurations considered in the power system as well as the number of buses, loads, and generators in each configuration are shown in Table 2.

In each configuration, 1000 different loading levels are produced in the range of 50-150% of the initial load values using the method described in Section 3. For example, P-V curves of load bus 3 at the base loading level of configurations 1 and 3 are shown in Fig. 4 and the following can be stated:

- When ignoring the AVR voltage limit of the generating units in the power system (unlimited power system), the voltage stability margin of the power system in configurations 1 and 3 will be 4872 and 3529 MW, respectively. However, considering the constraint (18) (limited power system) decreases the voltage stability margin of the power system to 2428 and 1245 MW in configurations 1 and 3, respectively.
- In configuration 1, the AVR voltage of buses of 30, 31 and 32 are saturated and the type of voltage collapse point is SLIB. Whereas, the type of voltage collapse point in configuration 3 is SNB, in which the AVR voltage of buses of 30 and 32 are saturated.

The voltage stability margin indices of the limited power system shown in Fig. 4 are stored as the desired output of a pattern for the corresponding neural network module. As a result, for each neural network module, 1000 patterns are generated at different loading levels. Of these, 70% are used for training, 15% for validation, and the remaining 15% for corresponding neural network module testing. The choice of training, validation and testing patterns is done randomly. The number of neurons in the hidden layer for all neural network modules is considered to be 12. Training process of neural network modules is stopped when the termination criterion is satisfied or when a maximum number of 1000 epochs is achieved. The termination criterion for improving generalization of neural network modules is called early stopping. When the error on the validation set increases for 10 iterations, the training process is stopped, and weights and biases are returned in the minimum validation error. The minimum and maximum values of the different input and output variables to normalize the neural network modules database are listed in Table 3.

Eq. (24) is used to normalize the variable $v$.

$$v^n = \frac{v - v^{min}}{v^{max} - v^{min}} \tag{24}$$

where, $v^n$, $v^{min}$ and $v^{max}$ are the normalized, minimum and maximum values of the variable $v$.

The percent relative error (PRE) between actual and estimated solutions for the $i$th loading level in the $k$th configuration is calculated as follows:

$$PRE = \frac{VSPI_{i,k}^{act} - VSPI_{i,k}^{est}}{VSPI_{i,k}^{act}} \times 100 \tag{25}$$

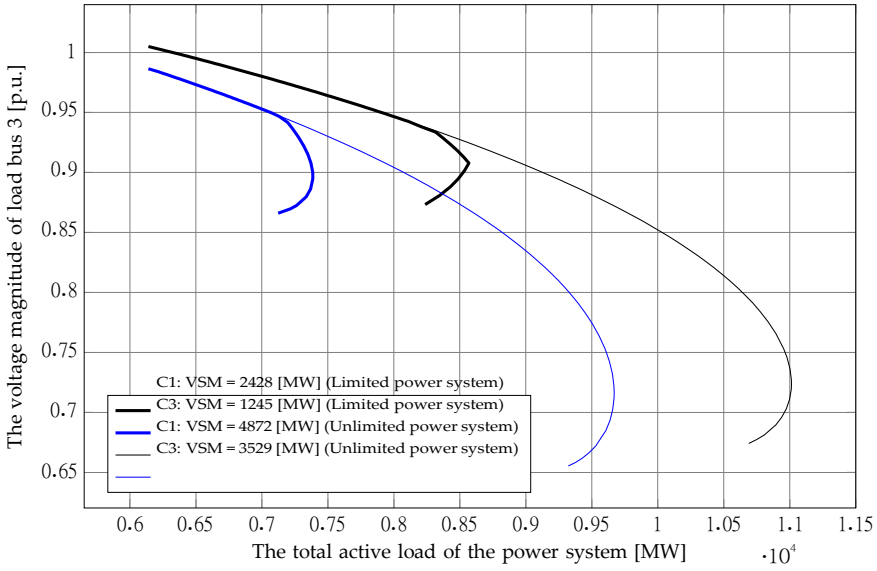


**Fig. 4** The sample P-V curves of load bus 3 in configurations 1 and 3.

**Table 3** The minimum and maximum values of the different input and output variables.

| | | C1 | C2 | C3 | C4 | C5 | C6 | C7 | C8 | C9 | C10 |
|---|---|---|---|---|---|---|---|---|---|---|---|
| $P_L$ | min | 4.2534 | 4.2532 | 4.2526 | 4.2526 | 4.2523 | 4.2601 | 4.2593 | 4.2568 | 4.2526 | 4.2601 |
| | max | 1655.7 | 1654.3 | 1653.5 | 1653.5 | 1655.9 | 1652.2 | 1655.9 | 1655.0 | 1653.5 | 1652.2 |
| $Q_L$ | min | 13.850 | 13.831 | 13.807 | 13.807 | 13.868 | 13.849 | 13.806 | 13.804 | 13.807 | 13.849 |
| | max | 374.94 | 374.61 | 374.43 | 374.43 | 374.99 | 374.15 | 374.98 | 374.77 | 374.43 | 374.15 |
| $P_G$ | min | 174.65 | 149.58 | 198.34 | 193.82 | 194.17 | 187.10 | 72.46 | 190.24 | 190.05 | 371.50 |
| | max | 1254.4 | 1477.9 | 1377.1 | 1379.1 | 1367.4 | 1375.6 | 1372.8 | 1344.1 | 1362.8 | 1287.3 |
| $V_r$ | min | 1.0274 | 1.0403 | 1.0367 | 1.0349 | 1.0347 | 1.0317 | 1.0313 | 1.0353 | 1.0304 | 1.0341 |
| | max | 4.9545 | 3.3510 | 5.3875 | 5.4794 | 5.4330 | 5.8779 | 3.1486 | 5.2725 | 5.3442 | 5.0907 |
| $E'_d$ | min | 0 | 0 | 0 | 0 | 0 | 0 | 0 | 0 | 0 | 0.0809 |
| | max | 0.6202 | 0.6002 | 0.6233 | 0.6215 | 0.6212 | 0.6129 | 0.5969 | 0.6285 | 0.6232 | 0.6191 |
| $E'_q$ | min | 0.8457 | 0.8513 | 0.8638 | 0.8616 | 0.8520 | 0.8523 | 0.8471 | 0.8457 | 0.8858 | 0.8844 |
| | max | 1.4533 | 1.3054 | 1.5288 | 1.5613 | 1.5522 | 1.7148 | 1.2566 | 1.5261 | 1.5299 | 1.3054 |
| $V$ | min | 0.9360 | 0.9165 | 0.8850 | 0.8812 | 0.9114 | 0.9256 | 0.9244 | 0.9342 | 0.9296 | 0.9232 |
| | max | 1.0578 | 1.0551 | 1.0528 | 1.0530 | 1.0553 | 1.0560 | 1.0570 | 1.0567 | 1.0522 | 1.0501 |
| $vsm$ | min | 720.69 | 144.82 | 139.39 | 156.14 | 177.92 | 224.51 | 359.10 | 438.10 | 351.34 | 468.94 |
| | max | 3575.4 | 2248.1 | 2612.0 | 2916.7 | 2939.5 | 3092.6 | 3021.0 | 3068.7 | 3039.6 | 3505.5 |

**Table 4** The minimum, mean and maximum of PRE for neural network modules.

| Module | Training phase | | | Validation phase | | | Testing phase | | |
|---|---|---|---|---|---|---|---|---|---|
| | min | mean | max | min | mean | max | min | mean | max |
| 1 | 1.42e-04 | 0.0825 | 2.3430 | 5.32e-04 | 0.1395 | 1.5757 | 0.0012 | 0.1433 | 1.1308 |
| 2 | 5.52e-07 | 0.0179 | 0.9670 | 1.41e-04 | 0.0507 | 1.3623 | 4.91e-05 | 0.0915 | 3.4324 |
| 3 | 1.42e-04 | 0.0623 | 2.4918 | 1.78e-04 | 0.1934 | 2.3153 | 5.33e-04 | 0.2525 | 3.7772 |
| 4 | 1.46e-04 | 0.0841 | 2.1321 | 8.00e-04 | 0.1983 | 2.6859 | 2.74e-04 | 0.1862 | 2.4526 |
| 5 | 7.41e-06 | 0.0116 | 0.2323 | 8.74e-04 | 0.0894 | 4.4944 | 1.49e-04 | 0.0500 | 0.9703 |
| 6 | 2.41e-05 | 0.0472 | 2.1172 | 6.03e-04 | 0.1407 | 3.9442 | 6.49e-04 | 0.1376 | 2.0481 |
| 7 | 1.47e-04 | 0.0411 | 1.0850 | 8.87e-04 | 0.1256 | 3.6228 | 8.21e-05 | 0.0954 | 1.8969 |
| 8 | 4.00e-05 | 0.0452 | 0.6881 | 4.99e-04 | 0.1262 | 2.9495 | 8.89e-05 | 0.1460 | 1.0408 |
| 9 | 1.10e-05 | 0.0640 | 2.3936 | 7.62e-04 | 0.1096 | 0.7934 | 6.10e-04 | 0.1077 | 2.6375 |
| 10 | 2.12e-05 | 0.0561 | 1.7862 | 3.89e-04 | 0.1496 | 2.6823 | 9.33e-04 | 0.1721 | 3.1040 |

where, $vsm_{i,k}^{act}$ is the voltage stability margin index obtained by the simultaneous equilibrium tracing technique and $vsm_{i,k}^{est}$ is the voltage stability margin index estimated by the neural network module.

Table 4 summarizes the simulation results in terms of the minimum, mean and maximum of PRE for each module in the training, validation and testing phases, respectively.

The results of implementing neural network method instead of the simultaneous equilibrium tracing technique are summa-

rized below:

**Table 5** The results of load shedding implementation at two sample loading levels in configuration 9.

| | | Loading level 1 | | | | | Loading level 2 | | | | |
|---|---|---|---|---|---|---|---|---|---|---|---|
| Bus number | $i$ | $P_{L_i}$ [MW] | $b_i$ | $a_i$ [%] | $P_{Shd_i}$ [MW] | $P_{L_i}^{new}$ [MW] | $P_{L_i}$ [MW] | $b_i$ | $a_i$ [%] | $P_{Shd_i}$ [MW] | $P_{L_i}^{new}$ [MW] |
| 3 | 1 | 480.4568 | 1 | 9.9267 | 47.6934 | 432.7634 | 476.0641 | 1 | 13.4897 | 64.2198 | 411.8443 |
| 4 | 2 | 742.9896 | 0 | 0 | 0 | 742.9896 | 694.1648 | 1 | 6.9795 | 48.4490 | 645.7158 |
| 7 | 3 | 171.9719 | 1 | 2.1261 | 3.6563 | 168.3156 | 193.1590 | 1 | 9.2229 | 17.8148 | 175.3442 |
| 8 | 4 | 510.7803 | 0 | 0 | 0 | 510.7803 | 638.4728 | 1 | 2.2727 | 14.5107 | 623.9621 |
| 12 | 5 | 11.5089 | 1 | 6.0850 | 0.7003 | 10.8086 | 7.7484 | 1 | 14.0176 | 1.0861 | 6.6622 |
| 15 | 6 | 303.9997 | 1 | 9.4575 | 28.7507 | 275.2490 | 325.0166 | 0 | 0 | 0 | 325.0166 |
| 16 | 7 | 271.4204 | 0 | 0 | 0 | 271.4204 | 335.1822 | 0 | 0 | 0 | 335.1822 |
| 18 | 8 | 218.5606 | 0 | 0 | 0 | 218.5606 | 145.7279 | 1 | 8.5337 | 12.4360 | 133.2919 |
| 20 | 9 | 988.6662 | 0 | 0 | 0 | 988.6662 | 830.1976 | 0 | 0 | 0 | 830.1976 |
| 21 | 10 | 221.8655 | 0 | 0 | 0 | 221.8655 | 319.491 | 1 | 0.9824 | 3.1387 | 316.3523 |
| 23 | 11 | 163.8197 | 0 | 0 | 0 | 163.8197 | 147.5395 | 0 | 0 | 0 | 147.5395 |
| 24 | 12 | 448.3771 | 0 | 0 | 0 | 448.3771 | 404.2654 | 1 | 3.3284 | 13.4558 | 390.8096 |
| 25 | 13 | 308.7882 | 1 | 4.2522 | 13.1303 | 295.6579 | 200.5778 | 0 | 0 | 0 | 200.5778 |
| 26 | 14 | 139.9967 | 0 | 0 | 0 | 139.9967 | 121.2222 | 1 | 6.5543 | 7.9452 | 113.2770 |
| 27 | 15 | 145.6267 | 1 | 5.6305 | 8.1995 | 137.4272 | 228.9683 | 1 | 0.2933 | 0.6715 | 228.2968 |
| 28 | 16 | 263.2999 | 0 | 0 | 0 | 263.2999 | 187.4401 | 0 | 0 | 0 | 187.4401 |
| 29 | 17 | 243.6561 | 0 | 0 | 0 | 243.6561 | 287.8585 | 1 | 1.6276 | 4.6851 | 283.1734 |
| 38 | 18 | 1408.2601 | 0 | 0 | 0 | 1408.2601 | 1592.192 | 0 | 0 | 0 | 1592.1920 |

**Table 6** The comparative results of voltage stability margin estimation at two sample loading levels in configuration 9.

| | Before load shedding implementation | | After load shedding implementation | |
|---|---|---|---|---|
| | Loading level 1 | Loading level 2 | Loading level 1 | Loading level 2 |
| $\sum_{i=1}^{l} P_{Li}^{new}$ [MW] | 7044.0445 | 7135.2883 | 6941.9140 | 6946.8756 |
| $\sum_{i=1}^{l} P_{Shd_i}$ [MW] | – | – | 102.1306 | 188.4128 |
| $vsm^{min}$ [MW] | 1056.6067 | 1070.2932 | 1041.2871 | 1042.0313 |
| $vsm^{act}$ [MW] | 915.6652 | 804.5947 | 1043.8388 | 1046.2737 |
| $vsm^{est}$ [MW] | 916.4208 | 808.0709 | 1043.1121 | 1049.8118 |
| $PRE$ [%] | 0.0825 | 0.4320 | 0.0696 | 0.3382 |

- According to the experimental results mentioned in (Amjady, 2003), in the estimation of the power system voltage stability margin index, maximum 5% error for the corrective actions is acceptable. The numerical results in Table 4 show the maximum error of less than 4.5% for the neural network modules. Therefore, trained neural network modules are appropriate for implementing the load shedding strategy.
- The voltage stability margin index is produced with the simultaneous equilibrium tracing technique ($\sigma = 0.001$) (Razmi et al., 2012) and trained neural network modules in about 145 and 0.05 seconds, respectively. Therefore, from the point of view of the response speed in implementing the load shedding strategy, the trained neural network modules perform much better than the simultaneous equilibrium tracing technique.

According to the power system conditions, one of the trained neural network modules is selected to estimate the voltage stability margin of the power system. If the index produced by the neural network module is less than a predefined value, the load shedding algorithm is implemented. In this paper, the minimum voltage stability margin index of the power system is assumed to be 15% of the total active power system load at the relevant loading level. In each subpopulation, a binary genetic algorithm (Haupt and Ellen Haupt, 2004) with single point crossover, tournament selection, crossover rate of 0.85, mutation rate of 0.15, migration rate of 0.2 and deme size of 60 is used. Individuals migrate after every 25 generations and the algorithm stops in each processor after 200 iterations. A system of 5-processor with distributed-shared-memory implements the parallel program. All processors can access all of the memory that is physically distributed as a shared address space (Wang and Singh, 2009). The Message Pass Interface (MPI) (Snir et al., 1998) has been used as a communication protocol in parallel implementation. Parallel time, serial time, synchronization time, and communication time are four parts of the parallel program execution time (Gubbala and Singh, 1995). According to the results, proposed multiple-deme parallel genetic algorithm implements about 4 times faster than traditional single-population genetic algorithm.

For example, in configuration 9 and at two different loading levels, the load shedding algorithm is implemented. The results of load shedding at different load buses at these two loading levels are presented in Table 5. Also, the total load of the power system, the total load shed, the actual and estimated values of the voltage stability margin index and the percent relative error before and after load shedding implementation in these two loading levels are shown in Table 6. Based on the response obtained at the second loading level, the P-V curve for load bus 3 is shown in Fig. 5 after load shedding implementation. In addition, the output voltage and reference voltage curves of the AVR of generators in buses 30, 31 and 32 are shown in Figs. 6 and 7, respectively, after load shedding implementation. In Figs. 5-7, less thick curves are obtained when the AVR output voltage limits are not taken into account and are shown to better describe the problem.

By evaluating the results of the above tables and figures, the following conclusions can be achieved:

- At the first loading level, buses 3, 7, 12, 15, 25 and 27 and at the second loading level, buses 3, 4, 7, 8, 12, 18, 21, 24, 26, 27 and 29 as candidate buses for load shedding have been selected. As a result, in a given configuration, the load

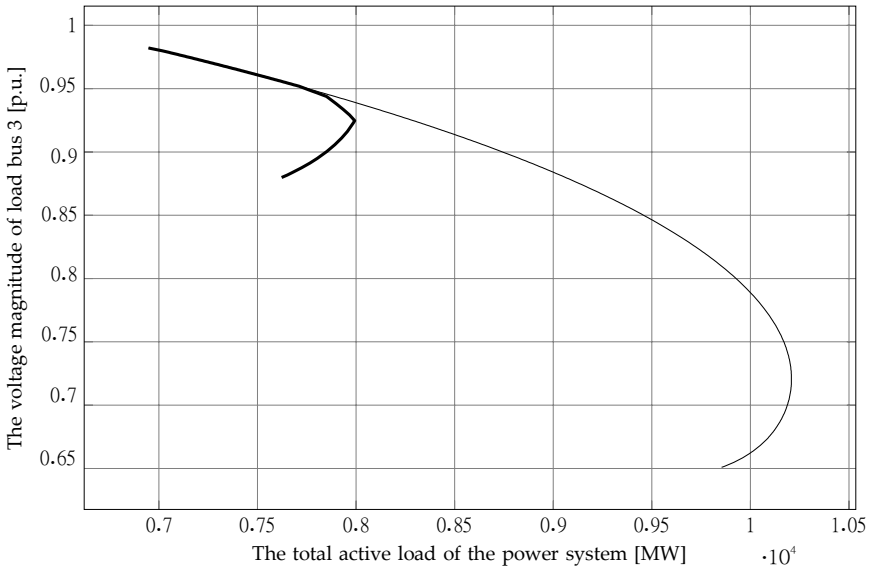


**Fig. 5** The P-V curve at loading level 2 in configuration 9 after load shedding implementation.

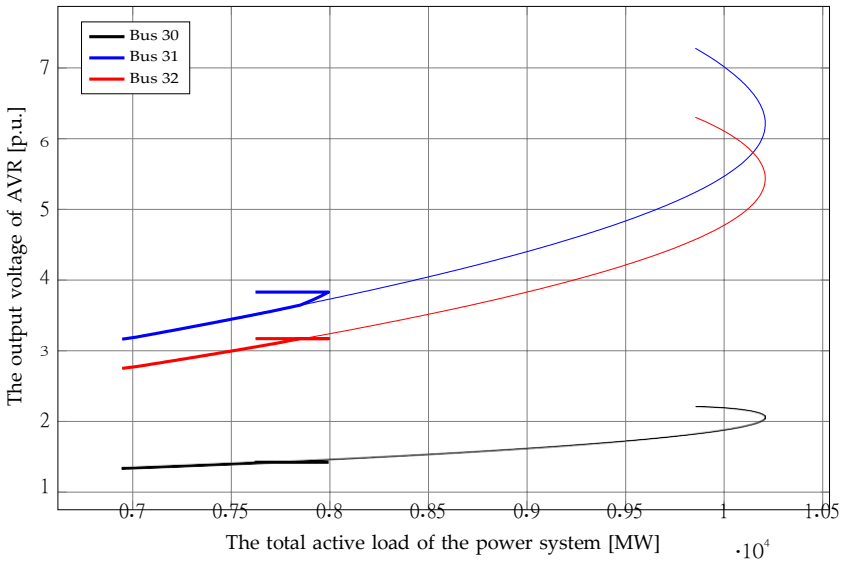


**Fig. 6** The output voltage of AVRs at loading level 2 in configuration 9 after load shedding implementation.

buses for load shedding will vary with changing the loading level, and cannot be considered specific buses before load shedding implementation.

- At the second loading level, given that the total load of the power system is 7135.2883 MW, the minimum acceptable voltage margin index to the power system shall be 2932.1070 MW. Estimation of this index by the corresponding modular neural network is 7070.808 MW and as a result, it is necessary to implement the load shedding algorithm under these conditions. After removing 188.4128 MW of the power system load, the total system load will be 6946.8756 MW. After implementing the load shedding algorithm, the result of estimating the voltage stability margin of the power system by the modular neural network is within the acceptable range. Therefore, by removing 188.4128 MW from the total load of the power system, 241.6790 MW will be added to the voltage stability margin index of the power system.
- Comparison of the estimated and actual results of the voltage stability margin index before and after the load shedding implementation in the first and second loading levels shows a relative error of less than 0.5%. As a result, due to the generalizability of the NN method, high estimation accuracy of this method is evident even after implementing the load shedding algorithm.
- At the second loading level and after the load shedding algorithm implementation, the output voltage of the AVR is saturated at the generation buses 30, 32 and 31 at loads of 7710, 7850 and 7993 MW, respectively. In this case, the AVR output voltage is not saturated in other buses. As can be seen in Fig. 6, the AVR output voltage in buses 30, 32 and 31

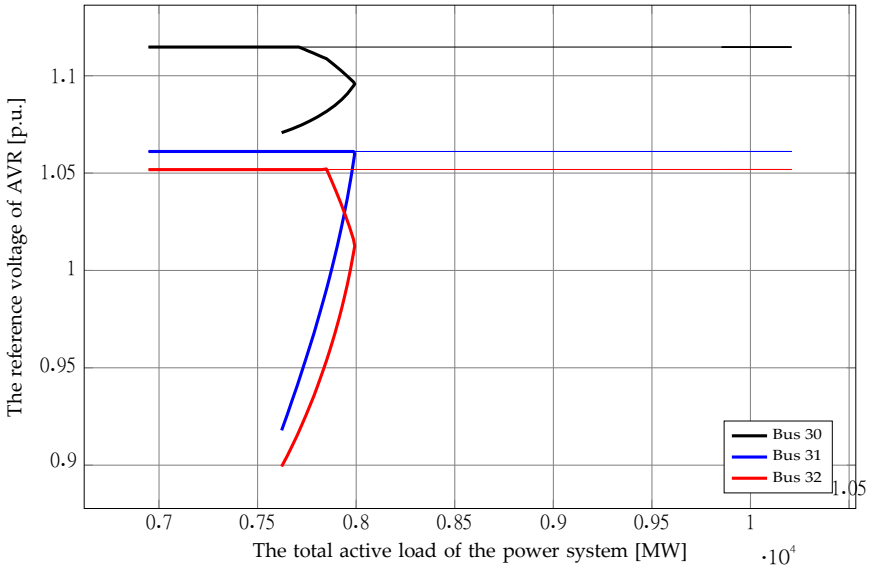


**Fig. 7** The reference voltage of AVRs at loading level 2 in configuration 9 after load shedding implementation.

**Table 7** The results of load shedding implementation at a sample loading level in configuration 2.

| Bus number | $i$ | $P_{L_i}$ [MW] | $b_i$ | $\alpha_i$ [%] | $P_{Shd_i}$ [MW] | $P_{L_i}^{new}$ [MW] |
|---|---|---|---|---|---|---|
| 3 | 1 | 464.6715 | 1 | 3.3431 | 15.5345 | 449.1370 |
| 4 | 2 | 742.0626 | 0 | 0 | 0 | 742.0626 |
| 7 | 3 | 137.2001 | 0 | 0 | 0 | 137.2001 |
| 8 | 4 | 449.0967 | 0 | 13.9296 | 62.5575 | 386.5392 |
| 12 | 5 | 11.6723 | 1 | 14.3109 | 1.6704 | 10.0019 |
| 15 | 6 | 367.4597 | 1 | 0 | 0 | 367.4597 |
| 16 | 7 | 302.2040 | 0 | 0 | 0 | 302.2040 |
| 18 | 8 | 235.3386 | 0 | 0 | 0 | 235.3386 |
| 19 | 9 | 240.8456 | 1 | 14.3548 | 34.5730 | 206.2726 |
| 21 | 10 | 276.3981 | 0 | 0 | 0 | 276.3981 |
| 22 | 11 | 280.1888 | 0 | 0 | 0 | 280.1888 |
| 23 | 12 | 251.8855 | 0 | 0 | 0 | 251.8855 |
| 24 | 13 | 153.8622 | 0 | 0 | 0 | 153.8622 |
| 25 | 14 | 366.7827 | 0 | 0 | 0 | 366.7827 |
| 26 | 15 | 224.7146 | 0 | 0 | 0 | 224.7146 |
| 27 | 16 | 219.1034 | 1 | 13.8123 | 30.2633 | 188.8401 |
| 35 | 17 | 1101.8286 | 0 | 0 | 0 | 1101.8286 |

increased to their maximum values of 1.43, 3.17 and 3.83 p.u., respectively and then remain constant at these numbers. From Fig. 7, it is clear that the AVR reference voltage at the generation buses 30, 32 and 31 are constant up to loads of 7710, 7850 and 7993 MW, respectively. After these values, the AVR reference voltage is reduced in these buses. The reason of this problem is because of the saturation of the AVR output voltage. Therefore, these state variables should be removed from the set of power system equations and, as a result of increasing the load and finding a new equilibrium point, it is necessary to replace the AVR reference voltage in these buses. As can be seen in Fig. 5, although the effect of AVR output voltage saturation on the generation bus 30 on the amplitude of voltage curve of load bus 3 is negligible, the AVR output voltage saturation on bus 32 has reduced the amplitude of voltage curve of load bus 3. Therefore, the AVR output voltage saturation of these two buses does not cause voltage instability when the operating point of the system still belongs to the upper part of the P-V curves. In other words, in this case only the voltage stability of the power system is destroyed, but the power system is still stable. By increasing the system load to 7993 MW again, the AVR output voltage is saturated at the generation bus 31. The saturation of this AVR changes the direction of the P-V curve and, in fact, the system operating point enters the unstable part of the P-V curves. Therefore, the AVR output voltage saturation on the generation bus 31 causes the power system to voltage collapse. As a result, the type of voltage collapse point is SLIB.

In Table 7, the values of active power loads at a sample loading level in configurations 2 are shown before and after the load shedding implementation by the multiple-deme parallel genetic algorithm method. In addition, the results obtained by applying the optimization algorithm in terms of sum of shed loads, the actual and estimated voltage stability margin index and the percent relative error are presented in Table 8. The convergence curve of this algorithm is also shown in Fig. 8. It should be noted that the results obtained after performing the optimization algorithm on several runs were not significantly different and an average state is shown in Fig. 8.

**Table 8** The results of voltage stability margin index estimation at a sample loading level in configuration 2.

| | Before load shedding implementation | After load shedding implementation |
|---|---|---|
| $\sum_{i=1}^{l} P_{Li}^{new}$ [MW] | 5825.315 | 5680.716 |
| $\sum_{i=1}^{l} P_{Shd_i}$ [MW] | – | 144.5987 |
| $vsm^{min}$ [MW] | 873.7973 | 852.1074 |
| $vsm^{act}$ [MW] | 691.2608 | 842.5251 |
| $vsm^{est}$ [MW] | 691.2158 | 852.2706 |
| *PRE* [%] | 0.0065 | 1.1567 |

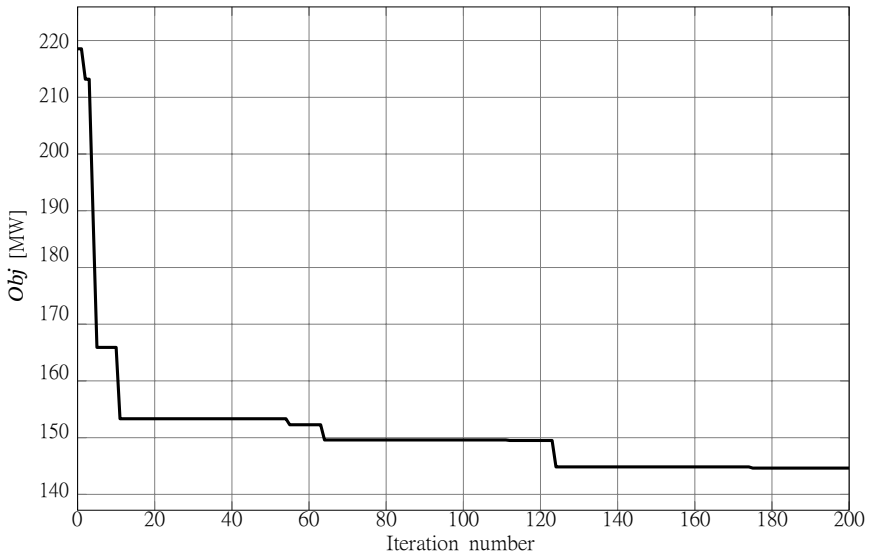


**Fig. 8** Convergence curve.

The results of Tables 7 and 8 and Fig. 8 can be summarized in the following items:

- The amount of load shed using the multiple-deme parallel genetic algorithm is about 2.5 MW and the proposed algorithm converges to the optimal solution after 124 iterations.
- The exact values of the voltage stability margin index using the solution obtained from the multiple-deme parallel genetic algorithm before and after the load shedding implementation are 691.2608 and 5251.842 MW, respectively. As a result, the voltage stability margin estimation by the corresponding neural network module has a relative error of 0.0065 and 1.1567%, respectively.
- In the case of the using the multiple-deme parallel genetic algorithm, with 144.5987 MW load shed in buses 3, 8, 12, 19 and 27, the voltage stability margin increased by 151.2643 MW.

The conclusions obtained from these simulations are:

- Using the multiple population genetic algorithm compared to other single population algorithms results in the global searching capability improvement and faster convergence.
- By using appropriate operators in different subpopulations, the chance of being stuck at a local optimum is decreased. Moreover, due to the use of elitism in the migration and exchange of chromosomes, the existence of an inappropriate operator in a subpopulation has no effect on finding the optimal solution.
- Because of the independence of the subpopulations from each other until the chromosomes are migrated, different operators can be used in each subpopulation.
- The performance of the proposed algorithm is 4 times faster than the single population type because of the added parallel processing capability.

## 6 Conclusion

In this paper, the multiple-deme parallel genetic algorithm was used to implement the load shedding strategy when the voltage stability margin of the power system is low. A modular neural network was introduced to fast estimate the voltage stability margin index of the power system. In each power system configuration, a neural network module was trained using power system operating conditions as input and the voltage stability margin index obtained by the simultaneous equilibrium tracing technique as the desired output under different loading conditions. The simultaneous equilibrium tracing technique

has the ability to accurately calculate the voltage stability margin index by defining complete components of generating units and taking into account the output voltage limit of AVRs. The proposed method has been tested on the New England 39-bus power system. The benefits of the proposed algorithm include higher speed and efficiency, additional CPU availability, more resistance to premature convergence and maintaining larger diversity.

**Acknowledgements** No funding is provided for the preparation of manuscript.

## Declarations

**Author contributions** All authors contributed to the study conception and design. Material preparation, data collection and analysis were performed by Dr. Hadi Razmi and Ali Gholami-Rahimabadi. The first draft of the manuscript was written by Dr. Hasan Doagou-Mojarrad and all authors commented on previous versions of the manuscript. All authors read and approved the final manuscript.

**Conflict of interest** The authors declare that they have no conflict of interest.

**Ethical approval** This article does not contain any studies with human participants or animals performed by any of the authors.

**Supplementary Information & ESM** Not applicable.

**Data Availability** Not applicable.

## References

Ahmadi A, Alinejad-Beromi Y (2015) A new integer-value modeling of optimal load shedding to prevent voltage instability. International Journal of Electrical Power & Energy Systems 65:210 – 219

Aman M, Arshad M, Zuberi H, Laghari J (2019) A hybrid scheme of load shedding using globalized frequency and localized voltage (GFLV) controller. International Journal of Electrical Power & Energy Systems 113:674 – 685

Amjady N (2003) Dynamic voltage security assessment by a neural network based method. Electric Power Systems Research 66(3):215 – 226

Amraee T, Ranjbar A, Mozafari B, Sadati N (2007) An enhanced under-voltage load-shedding scheme to provide voltage stability. Electric power systems research 77(8):1038 – 1046

Arya L, Koshti A (2014) Anticipatory load shedding for line overload alleviation using teaching learning based optimization (TLBO). International Journal of Electrical Power & Energy Systems 63:862 – 877

Arya L, Singh P, Titare L (2012a) Differential evolution applied for anticipatory load shedding with voltage stability considerations. International Journal of Electrical Power & Energy Systems 42(1):644 – 652

Arya L, Singh P, Titare L (2012b) Optimum load shedding based on sensitivity to enhance static voltage stability using DE. Swarm and Evolutionary Computation 6:25 – 38

Asrari A, Lotfifard S, Ansari M (2016) Reconfiguration of smart distribution systems with time varying loads using parallel computing. IEEE Transactions on Smart Grid 7(6):2713 – 2723

Babalola AA, Belkacemi R, Zarrabian S, Craven R (2017) Adaptive immune system reinforcement learning-based algorithm for real-time cascading failures prevention. Engineering Applications of Artificial Intelligence 57:118 – 133

Bakar NNA, Hassan MY, Sulaima MF, Na' im Mohd Nasir M, Khamis A (2017) Microgrid and load shedding scheme during islanded mode: A review. Renewable and Sustainable Energy Reviews 71:161 – 169

Bora TC, Mariani VC, dos Santos Coelho L (2019) Multi-objective optimization of the environmental-economic dispatch with reinforcement learning based on non-dominated sorting genetic algorithm. Applied Thermal Engineering 146:688 – 700

Dey B, Bhattacharyya B, Srivastava A, Shivam K (2019) Solving energy management of renewable integrated microgrid systems using crow search algorithm. Soft Computing pp 1 – 22

Gubbala N, Singh C (1995) Models and considerations for parallel implementation of Monte Carlo simulation methods for power system reliability evaluation. IEEE Transactions on Power Systems 10(2):779 – 787

Haupt RL, Ellen Haupt S (2004) Practical genetic algorithms

Hazra J, Sinha AK (2007) Congestion management using multiobjective particle swarm optimization. IEEE Transactions on Power Systems 22(4):1726 – 1734

Hooshmand R, Moazzami M (2012) Optimal design of adaptive under frequency load shedding using artificial neural networks in isolated power system. International Journal of Electrical Power & Energy Systems 42(1):220 – 228

Hosseini-Bioki M, Rashidinejad M, Abdollahi A (2013) An implementation of particle swarm optimization to evaluate optimal under-voltage load shedding in competitive electricity markets. Journal of Power Sources 242:122 – 131

Jalali A, Sepasian MS, Sheikh-El-Eslami MK (2019) Undisruptive load curtailment scheme to ensure voltage stability margin. IET Generation, Transmission & Distribution 13(9):1509 – 1519

Javadi M, Amraee T (2018) Mixed integer linear formulation for undervoltage load shedding to provide voltage stability. IET Generation, Transmission & Distribution 12(9):2095 – 2104

Kaffashan I, Amraee T (2015) Probabilistic undervoltage load shedding using point estimate method. IET Generation, Transmission & Distribution 9(15):2234 – 2244
Kanimozhi R, Selvi K, Balaji K (2014) Multi-objective approach for load shedding based on voltage stability index consideration. Alexandria Engineering Journal 53(4):817 – 825
Khamis A, Shareef H, Mohamed A, Dong ZY (2018) A load shedding scheme for DG integrated islanded power system utilizing backtracking search algorithm. Ain Shams Engineering Journal 9(1):161 – 172
Kucuktezcan CF, Genc VI (2015) Preventive and corrective control applications in power systems via big bang – big crunch optimization. International Journal of Electrical Power & Energy Systems 67:114 – 124
Lee CS, Ayala HVH, dos Santos Coelho L (2015) Capacitor placement of distribution systems using particle swarm optimization approaches. International Journal of Electrical Power & Energy Systems 64:839 – 851
Lei J, Li Y, Zhang B, Liu W (2014) A WAMS based adaptive load shedding control strategy using a novel index of transient voltage stability. In: Proceedings of the 33rd Chinese Control Conference, IEEE, pp 8164 – 8169
Li S, Wei Z, Ma Y (2018) Fuzzy load-shedding strategy considering photovoltaic output fluctuation characteristics and static voltage stability. Energies 11(4):779
Lim ZJ, Mustafa M (2016) Evolved intelligent clustered bee colony for voltage stability prediction on power transmission system. Soft Computing 20(8):3215 – 3230
Mageshvaran R, Jayabarathi T (2015a) GSO based optimization of steady state load shedding in power systems to mitigate blackout during generation contingencies. Ain Shams Engineering Journal 6(1):145 – 160
Mageshvaran R, Jayabarathi T (2015b) Steady state load shedding to mitigate blackout in power systems using an improved harmony search algorithm. Ain Shams Engineering Journal 6(3):819 – 834
Mahari A, Seyedi H (2016) A wide area synchrophasor-based load shedding scheme to prevent voltage collapse. International Journal of Electrical Power & Energy Systems 78:248 – 257
Mahdad B, Srairi K (2015) Blackout risk prevention in a smart grid based flexible optimal strategy using grey wolf-pattern search algorithms. Energy Conversion and Management 98:411 – 429
Moazzami M, Morshed MJ, Fekih A (2016) A new optimal unified power flow controller placement and load shedding coordination approach using the hybrid imperialist competitive algorithm-pattern search method for voltage collapse prevention in power system. International journal of electrical power & energy systems 79:263 – 274
Modarresi J, Gholipour E, Khodabakhshian A (2016) A comprehensive review of the voltage stability indices. Renewable and Sustainable Energy Reviews 63:1 – 12
Modarresi J, Gholipour E, Khodabakhshian A (2018) New adaptive and centralised under-voltage load shedding to prevent short-term voltage instability. IET Generation, Transmission & Distribution 12(11):2530 – 2538
Naganathan G, Babulal C (2019) Optimization of support vector machine parameters for voltage stability margin assessment in the deregulated power system. Soft Computing 23(20):10495 – 10507
Nojavan M, Seyedi H, Mohammadi-Ivatloo B (2017) Voltage stability margin improvement using hybrid non-linear programming and modified binary particle swarm optimisation algorithm considering optimal transmission line switching. IET Generation, Transmission & Distribution 12(4):815 – 823
Rahman MM, Ahmed A, Galib MMH, Moniruzzaman M (2021) Optimal damping for generalized unified power flow controller equipped single machine infinite bus system for addressing low frequency oscillation. ISA transactions
Razmi H, Shayanfar H, Teshnehlab M (2012) Steady state voltage stability with AVR voltage constraints. International Journal of Electrical Power & Energy Systems 43(1):650 – 659
Sadati N, Amraee T, Ranjbar A (2009) A global particle swarm-based-simulated annealing optimization technique for under-voltage load shedding problem. Applied Soft Computing 9(2):652 – 657
dos Santos Coelho L, Mariani VC (2007) Improved differential evolution algorithms for handling economic dispatch optimization with generator constraints. Energy conversion and management 48(5):1631 – 1639
Sapari N, Mokhlis H, Laghari JA, Bakar A, Dahalan M (2018) Application of load shedding schemes for distribution network connected with distributed generation: A review. Renewable and Sustainable Energy Reviews 82:858 – 867
Shekari T, Gholami A, Aminifar F, Sanaye-Pasand M (2016) An adaptive wide-area load shedding scheme incorporating power system real-time limitations. IEEE Systems Journal 12(1):759 – 767
Snir M, Gropp W, Otto S, Huss-Lederman S, Dongarra J, Walker D (1998) MPI – the Complete Reference: the MPI core, vol 1. MIT press
Suganyadevi M, Babulal C, Kalyani S (2016) Assessment of voltage stability margin by comparing various support vector regression models. Soft Computing 20(2):807 – 818
Tamilselvan V, Jayabarathi T (2016) A hybrid method for optimal load shedding and improving voltage stability. Ain Shams Engineering Journal 7(1):223 – 232
Tian A, Mou X (2019) A network analysis-based distributed load shedding strategy for voltage collapse prevention. IEEE Access 7:161375 – 161384
Titare L, Singh P, Arya L, Choube S (2014) Optimal reactive power rescheduling based on EPSDE algorithm to enhance static voltage stability. International Journal of Electrical Power & Energy Systems 63:588 – 599
Wang L, Singh C (2009) Multi-deme parallel genetic algorithm in reliability analysis of composite power systems. In: 2009 IEEE Bucharest PowerTech, IEEE, pp 1 – 6

Xia N, Gooi H, Abur A, Chen S, Eddy YF, Hu W (2016) Enhanced state estimator incorporating adaptive underfrequency load shedding under contingencies via the alternating optimization method. International Journal of Electrical Power & Energy Systems 81:239 – 247

Xu Y, Dong ZY, Luo F, Zhang R, Wong KP (2013) Parallel-differential evolution approach for optimal event-driven load shedding against voltage collapse in power systems. IET Generation, Transmission & Distribution 8(4):651 – 660